Vol 16 No 6, June 2007
1009-1963/2007/16(06)/1790-06
Chinese Physics
© 2007 Chin. Phys. Soc.
and IOP Publishing Ltd

Photoluminescence and electroluminescence properties of ZnO films on p-type silicon wafers*

Wang Fei-Fei(王菲菲)[a], Cao Li(曹 立)[a], Liu Rui-Bin(刘瑞斌)[a], Pan An-Lian(潘安练)[a], and Zou Bing-Suo(邹炳锁)[a)b)†]

[a] *Institute of Physics, Chinese Academy of Sciences, Beijing* 100080, *China*

[b] *Micro–Nano Technologies Research Center, Hunan University, Changsha* 410082, *China*

(Received 26 October 2006; revised manuscript received 29 December 2006)

A simplified n-ZnO/p-Si heterojunction has been prepared by growing n-type ZnO rods on p-type silicon wafer through the chemical vapour deposition method. The reflectance spectrum of the sample shows an independent absorption peak at 384 nm, which may be originated from the bound states at the junction. In the photoluminescence spectrum a new emission band is shown at 393 nm, besides the bandedge emission at 380 nm. The electroluminescence spectrum of the n-ZnO/p-Si heterojunction shows a stable yellow luminescence band centred at 560 nm，which can be attributed to the emission from trapped states. Another kind of discrete ZnO rod has also been prepared on such silicon wafer and is encapsulated with carbonated polystyrene for electroluminescence detection. This composite structure shows a weak ultraviolet electroluminescence band at 395 nm and a yellow electroluminescence band. These data prove that surface modification which blocks the transverse movement of carriers between neighbouring nanorods plays important roles in the ultraviolet emission of ZnO nanorods. These findings are vital for future display device design.

Keywords: ZnO, photoluminescence, electroluminescence
PACC: 7860F, 7855

1. Introduction

Wurtzite structured ZnO is an excellent luminescence material with large exciton binding energy (60 meV) and wide direct band gap. Recently, many papers have reported the growth of ZnO nanostructures on different substrates.[1−9] Though ZnO epitaxial films have shown excellent optical characteristics,[10−12] their electrical and electroluminescence properties have not been extensively studied. In 2004, Park *et al* reported the electroluminescence in n-ZnO nanorod arrays grown vertically on p-GaN.[13] Zhou also found the electroluminescence of n-ZnO/P-GaN heterojunction under both forward and reverse biases.[14] Furthermore, some researchers focused on the p-type doping in ZnO[15−18] in order to apply the ZnO p-n homojunction devices in daily life, for p-n homojunction devices could show a higher efficiency than heterojunction devices.[19,20] Although there are a lot of new findings, it is a long way to realize the electroluminescence application of ZnO-based devices because the device stability needs further improvement. In this paper, we report the deposition of ZnO on p-type silicon wafers by a chemical vapour deposition method and compare its luminescence properties with that reported by Park. Some special findings in our experiments may be important for future applications.

2. Experimental

ZnO film was synthesized in an electrical furnace with a horizontal quartz tube (35 mm in diameter, 100 cm in length). The source material contained equal amount (by weight) of pure ZnO and graphite powders, in which graphite powder was used to lower the growth temperature and reduce the zinc oxide to produce zinc vapour. These two kinds of powders were mixed together and thoroughly ground in an agate mortar. The silicon wafers used as substrates to collect samples were first cleaned with acetone in an ultrasonic bath, and then etched in 10% HF aqueous solution to remove the native oxide on their surfaces. After that, the silicon wafers were rinsed with de-

*Project supported by the National Natural Science Foundation of China (Grant No 20173073), National 973 Project (Grant No 2002CB713802), Nano- and Bio-device Key Project of CAS, 985 Project of Hunan University.
†E-mail: Zoubs@aphy.iphy.ac.cn

ionized water several times. Then the mixed powders were put into the centre of a small quartz tube with a special shape, and two pieces of clean silicon wafers were laid on both sides of the powder location. The small quartz tube was then transferred into the centre of the tube furnace when the central temperature of the furnace was 900 °C. The temperature was further raised to 1000 °C and kept this temperature for an hour. After that, the furnace power was turned off. When the furnace temperature was about 650 °C, the small quartz tube was taken out from the furnace and cooled down naturally. Finally, a white deposition film on the silicon wafer was observed after the quartz tube was cooled down to room temperature.

The as-synthesized product was characterized by scanning electron microscopy (SEM, Hitachi, S-4200) and x-ray diffractometer (XRD) (Japan, Rigaku, D/MAX-2400) equipped with graphite-monochromatized Cu $K\alpha$ radiation ($\lambda = 1.54178$ Å). A TU-1901 UV-Vis absorption spectrometer and a PTI-C-700 fluorescence spectrometer were used to obtain the reflectance and emission spectra of the sample. A CW He-Cd laser (50 mW, wavelength at 325 nm, IK 3552R-G) was used to measure the photoluminescence (PL) of the ZnO film on silicon wafer. The electroluminescence (EL) was measured by applying a direct current voltage to the heterojunction using a source meter (Keithley 2400). The EL spectra were measured using a monochromator, a detection system equipped with a photomultiplier tube and a photon counter was used for PL measurement. All measurements were performed at room temperature.

3. Results and discussion

Figure 1 shows the typical SEM image of ZnO film grown on p-type silicon wafers. Figures 1(a) and 1(b) are the images of the samples in high (sample A) and low (sample B) temperature regions, respectively. Figure 1(a) shows clearly that ZnO film with rod-like structure covers the whole surface of silicon wafer. Though the rods are not exactly perpendicular to the wafer surface, they have a tendency to grow normal to the substrate. The diameters of the rods range from about 10 to 40 μm. The inset is the cross-sectional image of the sample. It can be seen from the image that the rods connect with each other at the bottom of them. Figure 1 (b) is the sample grown in the low temperature region. Compared with sample A, the diameters of the rods in sample B are small and are almost discrete and perpendicular to the substrate. Figure 1(c) shows the XRD pattern of sample A. All diffraction peaks match with the standard data of hexagonal structure of ZnO (JCPDS 36-1451). The stronger (002) diffraction peak indicates that (001) is the preferred growth direction.

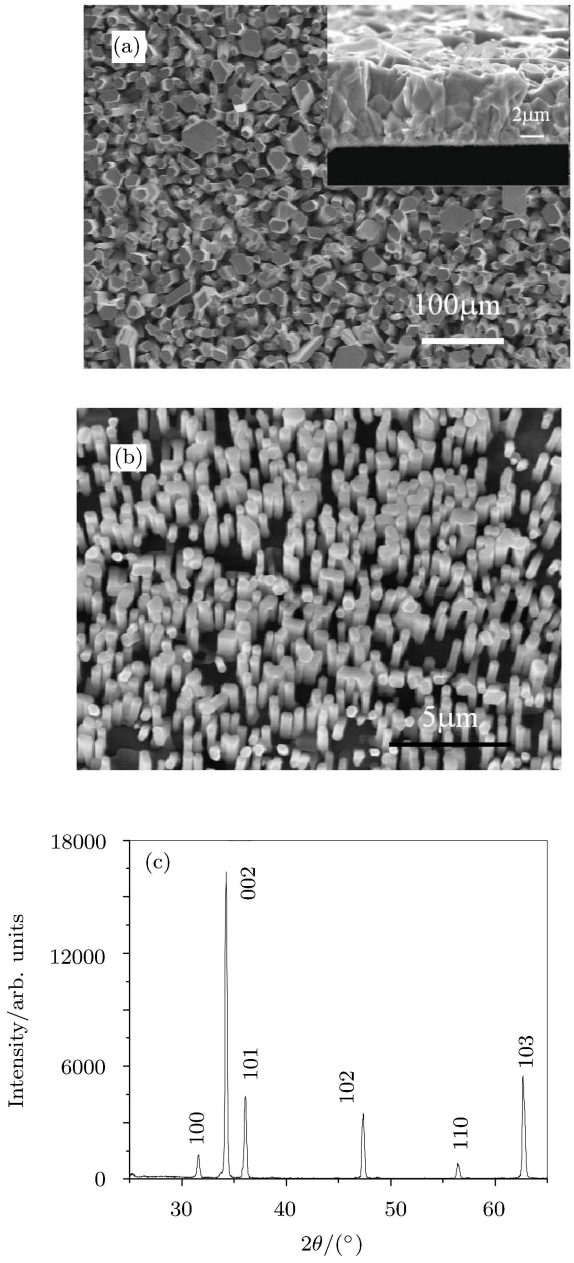


Fig.1. (a) and (b) SEM images of ZnO films grown on silicon wafers; the inset in (a) is the sectional view of the sample. (c) XRD pattern of the sample shown in (a).

Samples A and B show similar PL characteristics. Figure 2(a) shows the typical PL and reflectance spectra of sample A. From Fig.2(a) three bands can be seen centred at 380 nm (3.26 eV), 393 nm (3.16 eV) and 486 nm (2.55 eV). The UV emission band

at 380 nm can be attributed to the free exciton emission at near band-edge[21] and the emission at 393 nm is induced by the bound excitons.[22,23] At the heterojunction interface, some shallow bound states (the junction state) are formed by the infiltration of p-Si and n-ZnO at high temperatures. The green emission band centred at 486 nm is usually believed to originate from various surface defects, such as the singly ionized oxygen vacancies and interstitial zinc atoms.[24,25] It is interesting to note that under a long-time UV light illumination, the emission band at 393 nm will enhance gradually while the band at 380nm is weakened with time evolution as shown in Fig.2(b). This may be caused by carrier movement and thermal repopulation of electronic states, i.e. a carrier movement process to the bound states near the junction in this thick ZnO film. The higher temperature caused by laser excitation makes the holes in the valence band (electrons in the conduction band) gradually relax to the bound junction states, leading to a stronger emission band at 393 nm. If the sample is once again excited after a few minutes' break, this phenomenon will appear again.

The inset in Fig.2(a) is the reflectance spectrum of ZnO on silicon wafer as compared with that of pure ZnO sample. The reflectance spectrum of the composite film shows an independent absorption peak at 384 nm, while that of pure ZnO only shows a sharp absorption edge. The knee point at about 375 nm for the pure ZnO spectrum indicates its intrinsic bandgap and the obvious absorption peak at 384 nm in the composite film might be caused by the bound junction states near the junction interface. Moreover, the 'valley' at 375 nm shows a clear separation between continuum band and bound states.

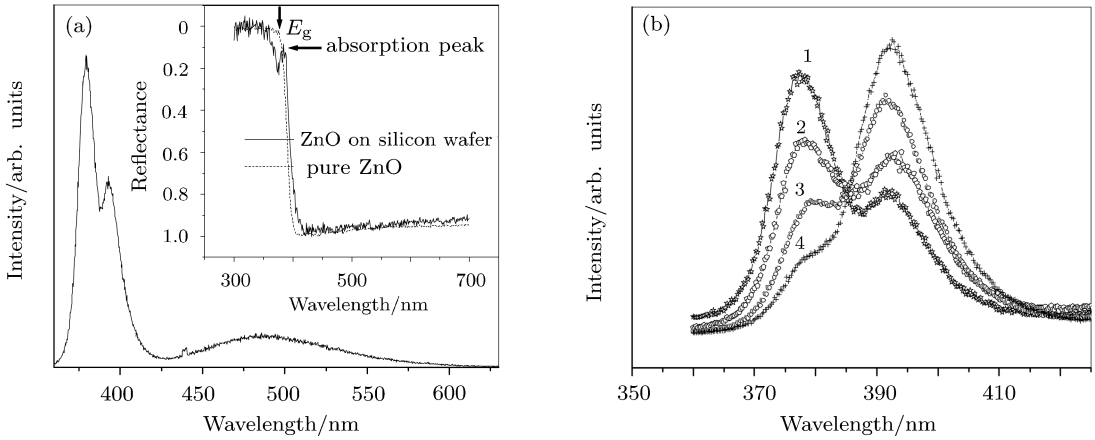


Fig.2. The PL spectrum of ZnO on silicon wafer; the inset is the reflectance spectra of it and pure ZnO (without substrate). (b) The change of PL spectra of ZnO on silicon wafers with increasing illuminating time from 1 to 4.

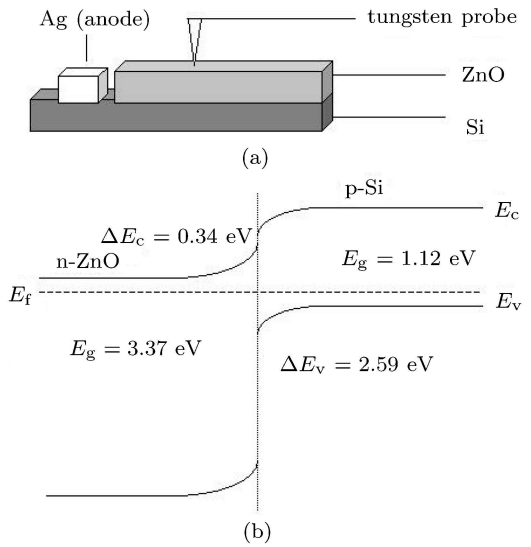


Fig.3. (a) Schematic diagram of n-ZnO/p-Si heterojunction, and (b) band diagram of the heterojunction.

A schematic diagram of n-ZnO/p-Si heterojunction is shown in Fig.3(a). A large area ohmic-contact of silver glue is placed on the silicon surface to provide a low contact resistance of electrode, and a tungsten probe is put on the surface of ZnO. Figure 3(b) shows the 'ideal' band diagram of the n-ZnO/p-Si structure. The electron affinities (χ) of ZnO and silicon are assumed to be 4.35[26] and 4.01 eV. The band gaps of ZnO and silicon at room temperature are 3.37 and 1.12 eV, respectively. So the energy barrier ΔE_C for an electron is $\Delta E_C = \chi(\mathrm{Si}) - \chi(\mathrm{ZnO}) = 4.01 - 4.35 = -0.34$ eV, and the energy barrier ΔE_V for a hole is $\Delta E_V = E_g(\mathrm{Si}) + \Delta E_C - E_g(\mathrm{ZnO}) = 1.12 - 0.34 - 3.37 = -2.59$ eV. Due to different electron affinities and the band gaps of ZnO and silicon, there are two energy band offsets. Electrons and holes can accumulate at

the interface because of the conduction and valence band offsets. The band alignment of silicon and ZnO suggests that the barrier for holes transport is higher than that for electron transport when applying a forward bias voltage, so a significant amount of direct recombination may be expected to occur non-radiatively in the silicon layer. However, light emission have been observed in the n-CdS/p-Si core/shell structure. [27] Since the band alignment of n-ZnO/p-Si is similar to that of n-CdS/p-Si, light emission is expected to occur in n-ZnO/p-Si structure.

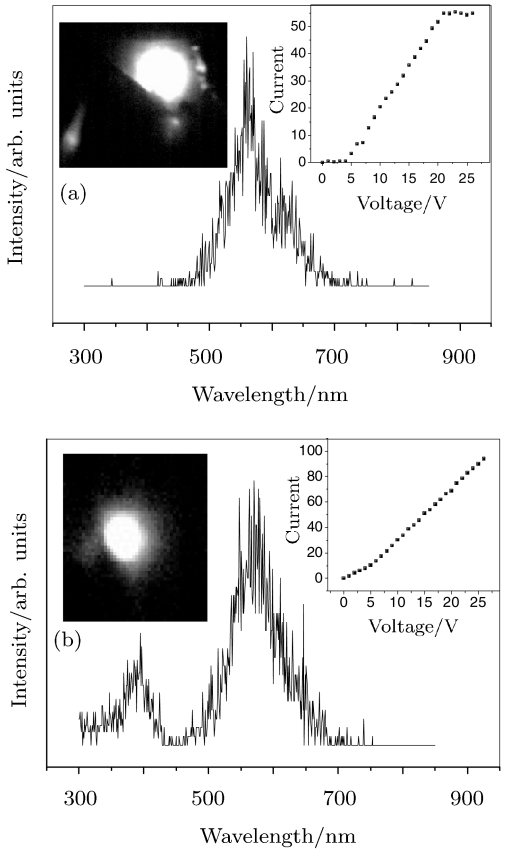


Fig.4. The EL spectra of sample A (a) and sample B (b). The insets are the EL images from the heterojunctions and their *I-V* curves.

Figure 4(a) is the EL spectrum of sample A at room temperature when applying a forward bias greater than the band gap of ZnO to the p-n junction. The insets are the EL image and light emission intensity versus the voltage applied to the heterojunction. The EL is strong enough to be observed with the naked eye, and the central wavelength is about 560 nm, which is the emission of the trapped state near the junction. Some important conclusions could be drawn from the experimental processes. First, the light emission can be seen when the forward bias is about 6 V. When the applied voltage exceeds the threshold, the radiative recombination of electron/hole pairs occurs.[28] Second, above the threshold the current presents an almost linear increasing dependence on the voltage and saturated at about 22 V (see the inset in Fig.4(a)). Finally, stable light emission can last about 30 min in air at room temperature when applying a forward bias of 10 V and is weakened gradually probably due to the thermal damage to the junction.

The threshold voltage of the heterojunction is higher than the band gap of ZnO, which may be due to the large series resistance of this structure. Furthermore, the carrier loss via transverse transport in the ZnO layer could also lead to a higher threshold voltage. An evidence for transverse transport between neighbouring nanorods is that several obvious emission spots far from the electrode site (about 1 cm) can be observed on the ZnO film (see the inset in Fig.4(a)). This clearly indicates that the injected carriers can move along two directions, transversely along the surface and longitudinally through the junction. The transverse and longitudinal movements and distribution of carriers cause the luminescence site to move away from the location of the electrode.

In the n-ZnO/p-GaN heterojunction,[13] Park used photoresist to block the transverse transport and obtained a low threshold emission. When the voltage increases to a certain value, a higher-energy-level emission can be observed. In our comparison experiment, discrete ZnO rods on silicon wafers were also prepared as shown in Fig.1(b). By filling the free space between nanorods with carbonated polystyrene, we found that the *I-V* curve in Fig.4(b) is similar to the results reported by Park[13] and Konenkamp.[29] A weak UV emission apart from the yellow emission occurs when we apply a large forward voltage. So it can conclude from the experiments that the transverse transport between ZnO nanostructures is dominant in the relaxation of electron-injected excited states. It also leads to the less efficient emission and the dominant nonradiative recombination. Otherwise, the near band edge emission of ZnO should be observed. So the surface modification is very important and should be used to improve the UV emission in the EL of ZnO nanorod structures.

The graphs from (1) to (4) in Fig.5(a) and 5(b) are the simple illustrations of the carriers' movement in a discrete rod and the connected rods respectively with increasing applied voltage from 0 to 28 V. When the applied voltage increases, the carriers are injected

to higher energy level as illustrated in graphs from (1) to (4). For discrete nanorods, green emission appears when electrons are injected into the trapped states, and higher-energy-level emission (near band edge emission) can be observed by further increasing the applied voltage. Unlike the movements in a discrete rod, where the transverse transport is blocked by polymer and only longitudinal movement across the electrode, junction and rod is allowed, the carriers can move both longitudinally and transversely in connected rods as shown in Fig.5(b). And the electrons cannot be injected into the conduction band because of the loss due to the transverse movement of carriers and the trapped state. So, the UV emission cannot be observed in connected rods even at a higher voltage.

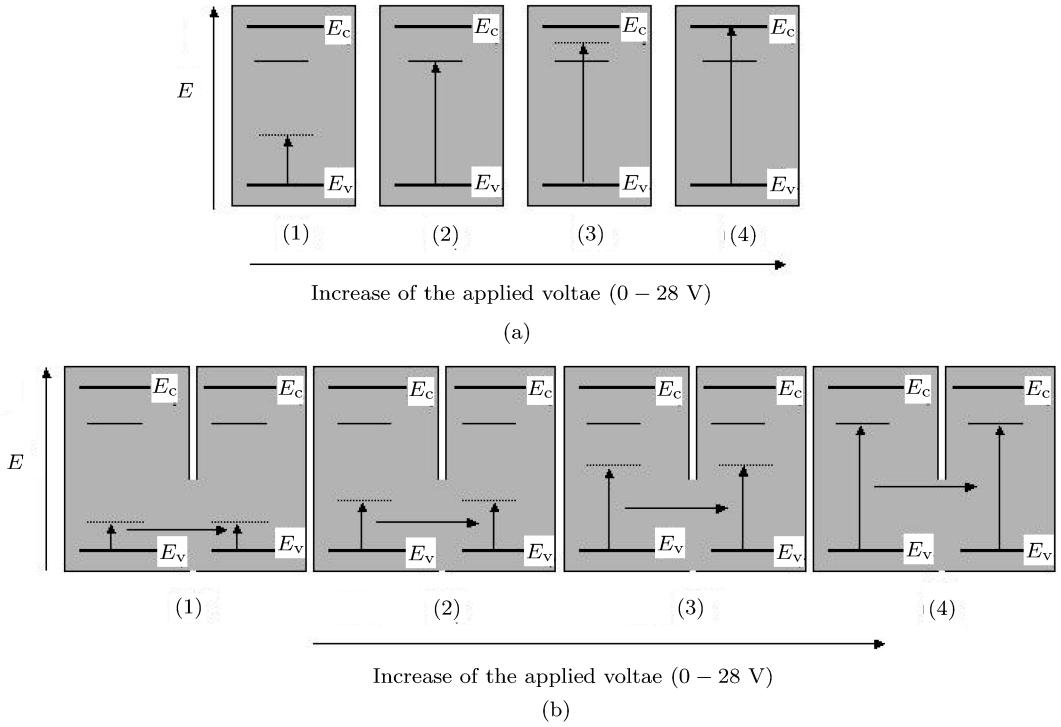


Fig.5. Illustrations of carriers' transports in discrete rods (a) and connected rods (b) with increasing applied voltage. The direction of arrows indicates the direction of carriers' movement.

4. Conclusions

In conclusion, a simplified n-ZnO/p-Si heterojunction have been fabricated by using a simple method. The PL of the sample shows three peaks at 385, 393 and 510 nm. The extraordinary peak centred at 393 nm may be due to the bound junction states caused by the interaction of silicon and ZnO. Though the heterojunction is not optimized, the device shows strong yellow EL at about 560 nm, which can be attributed to the emission of the trapped state, without the near band-edge emission of ZnO. By filling the free space of the discrete nanorods with polymer, the device shows weak UV emission band in its EL spectra. It can be concluded from the experimental data that the transverse transport between nanorods may be the dominant factor for the appearance of the trapped state emission only. If this transverse transport is blocked by polymer, the higher level can be populated for UV emission. So the surface modification is very important. These devices may be further optimized and have potential application in the display devices.

References

[1] Wang X D, Song J H, Li P, Ryou J H, Dupuis R D, Summers C J and Wang Z L 2005 *J. Am. Chem. Soc.* **127** 7920
[2] Yang R S and Wang Z L 2005 *Solid State Comm.* **134** 741
[3] Greene L, Law M, Goldberger J, Kim F, Johnson J, Zhang Y, Saykally R and Yang P 2003 *Angew. Chem. Int. Ed.*

42 3031
[4] Huang M, Wu Y, Feick H, Tran N, Weber E and Yang P 2001 *Adv. Mater.* **13** 113
[5] Könenkamp R, Word R C and Schlegel C 2004 *Appl. Phys. Lett.* **85** 6004
[6] Pauporte' T and Lincot D 1999 *Appl. Phys. Lett.* **75** 3817
[7] Zhang L L, Guo C X, Chen J G and Hu J T 2005 *Chin. Phys.***14** 586
[8] Wang Z J, Wang Z J, Li S C, Wang Z H, Lü Y M and Yuan J S 2004 *Chin. Phys.* **13** 750
[9] Zhang X T, Xiao Z Y, Zhang W L, Gao H, Wang Y X, Liu Y C, Zhang J Y and Xu W 2003 *Acta Phys. Sin.* **52** 740 (in Chinese)
[10] Huang M H, Mao S, Feick H, Yan H Q, Wu Y Y, Kind H, Weber E, Russo R and Yang P D 2001 *Science* **292** 1897
[11] Zu P, Tang Z K, Wong G K L, Kawasaki M, Ohtomo A, Koinuma H, Segawa Y and Seyawa Y 1997 *Solid State Commun.* **103** 459
[12] Jung S W, Park W I, Cheong H D, Yi G C, Jang H M, Hong S and Joo T 2002 *Appl. Phys. Lett.* **80** 1924
[13] Park W I and Yi G C 2004 *Adv.Mater.* **16** 87
[14] Qin Q, Guo L W, Zhou Z T, Chen H, Du X, Mei Z X, Jia J F, Xue Q K and Zhou J M 2005 *Chin. Phys. Lett.* **22** 2298
[15] Tsukazaki A, Onuma T, Ohtani M, Makino T, Sumiya M, Ohtani K, Chichibu S F, Fuke S, Segawa Y, Ohno H, Koinuma H and Kawasaki M 2005 *Nat. Mater.* **4** 42
[16] Aoki T, Hatanaka Y and Look D C 2000 *Appl. Phys. Lett.* **76** 3257
[17] Guo X L, Choi J H, Tabata H and Kawai T 2001 *Jpn. J. Appl. Phys.* **Part 240** L177
[18] Tsukazaki A, Kubota M, Ohtomo A, Onuma T, Ohtani K, Ohno H, Chichibu S F and Kawasaki M 2005 *Jpn. J. Appl. Phys.* **Part 244** L643
[19] Duan X, Huang Y, Cui Y, Wang J and Lieber C M 2001 *Nature* **409** 66
[20] Duan X, Huang Y, Cui Y, Agarwal R and Lieber C M 2003 *Nature* **421** 241
[21] Kong Y C, Yu D P, Zhang B, Fang W and Feng S Q 2001 *Appl. Phys. Lett.* **78** 407
[22] Choopun S, Vispute R D, Noch W, Balsamo A, Sharma R P and Venkatesan T 1999 *Appl. Phys. Lett.* **75** 3947
[23] Wong M H, Berenov A, Qi X, Kappers M J, Barber Z H, Illy B, Lockman Z, Ryan M P and MacManus-Driscoll J L 2003 *Nanotechnology* **14** 968
[24] Vanheusden K, Warren W L, Seager C H, Tallant D R, Voigt J A and Gnade B E 1996 *J. Appl. Phys.* **79** 7983
[25] Bylander E G 1978 *J. Appl. Phys.* **49** 1188
[26] Aranovich J A, Golmayo D G, Fahrenbruch A L and Bube R H 1980 *J. Appl. Phys.* **51** 4260
[27] Hayden O, Greytak A B and Bell D C 2005 *Adv. Mater.* **17** 701
[28] Huang Y, Duan X and Lieber C M 2005 *Small* **1** 142
[29] Konenkamp R, Word R C and Godinez M 2005 *Nano lett.* **5** 2005